https://doi.org/10.2352/CIC.2024.32.1.7

Estimating Spectral BRDF Parameters Using Handheld Devices

Bita Panahi, Aditya Sole, and Ivar Farup, Norwegian University of Science and Technology, Gjøvik, Norway.

Abstract

The Bidirectional Reflectance Distribution Function (BRDF) is one of the tools for characterising the appearance of real-world materials. However, bidirectional reflectance measurements and data processing can be time-consuming and challenging. This paper aims to estimate the BRDF values of eight matt samples using two portable, handheld devices, one for diffuse reflectance and one for specular reflectance measurements. The data is fitted to the Cook-Torrance BRDF model in the spectral domain to get the optimised parameters and the estimated spectral BRDF values using three different cost functions. The estimated BRDF is evaluated using a colour-difference metric. The results show that it would be possible to estimate spectral BRDF of a sample using measurements from two simple measurement devices having fewer angle combinations for both the diffuse and specular measurements. This results in a shorter measurement and processing time, lower storage usage, and estimations of spectral BRDF values. Moreover, the cube root cosine-weighted RMSE cost function shows more consistency in the colour reproduction estimated by the fitted BRDF model.

Introduction

When it comes to characterising and modelling the appearance of materials, the bidirectional reflectance distribution function (BRDF) is a tool that enables us to study the interaction of light with the surface and model the appearance based on this interaction. Using this function, it is possible to define the relationship between the incoming light and reflected light from different illumination and viewing angles. This process requires the angles of the illumination source and the detector to be precise concerning the orientation of the sample surface [1] and thus can be time-consuming and challenging [2].

BRDF measurements can be performed using different approaches. Image-based setups that include a digital camera as a sensor and a light source [3, 4] have the advantage of decreasing the cost and measurement duration, since multiple photos can be taken from the surface containing different surface orientations with respect to the illumination angle. The drawback of this method is that, in most cases, instead of spectral data, RGB data is obtained; therefore, it is not as precise as desired. Several studies have been done using this method for BRDF measurements, such as the work by Ngan et al. [5] in which they used a measurement setup for flexible and flat samples. In their setup, they used a light source that rotated around the sample holder, which was a cylinder with samples being wrapped around it, and data was captured using a camera in a fixed position. Another approach for BRDF measurements is to use a goniospectrophotometer. This technique gives us the spectral data of the reflected light from the surface in both diffuse and specular directions, depending on the design of the measurement device [2]. This setup consists of a light source, a detector, and a sample mounted onto a holder. The light source and/or detector rotates around the sample, resulting in the surface being illuminated and measured precisely at a relatively high angular resolution from different directions. This method can, however, be time-consuming and relatively expensive [6, 7, 8].

The obtained measurements can be used to fit various BRDF models that represent surface characteristics of the material [2]. Depending on the applications, phenomenological, physically-based, or data-driven BRDF models can be used. In phenomenological models, we use the reflectance data and fit it to the analytical equations [9]. The basis of physically-based models is physics and surface optics that assumes the surface as micro surfaces with different distributions in size and directions [2]. In data-driven models, instead of using theoretical functions to estimate the reflectance of the surface, the actual measured data at different illumination and viewing angles are used. Consequently, more realistic representations of the real-world materials would be feasible, although the data storage and processing have remained a challenge in this type of BRDF model [2, 10]. The challenges in BRDF measurements, estimations, and data storage have increased the need for fast and precise measurement procedures that can use a minimal and optimal digital storage space and processing time.

In this paper, we investigate measuring and estimating sample BRDF using portable handheld measurement device(s) that can perform fast directional spectral measurements at fewer angle combinations compared to the traditional goniospectrophotometers that cover the complete hemisphere. We use two handheld measurement devices to capture the diffuse and specular surface reflectance from the sample surface with fewer angle combinations. We optimise and evaluate a standard BRDF model using the obtained measurement data, three different cost functions, and a colour-difference metric for samples that show diffuse reflectance properties. The objectives of this work are as follows:

1. To use portable, handheld devices to measure and estimate BRDF values in the spectral domain with a lower number of angle combinations.
2. To evaluate the performance of different cost functions in the optimisation process of the BRDF parameters for the samples used in this paper.

Background

One of the most popular BRDF models, especially in computer graphics, is the Cook-Torrance model [11]. This model includes both the specular and diffuse reflections, and the specular lobe in this model is calculated using the halfway vector, h [2]. Cook-Torrance model is based on the microfacet theory, which means that we assume only the microfacets with the orientation towards the h are responsible for the final reflected light at θ_i. The angles and vectors of this model are shown in Figure 1.

The mathematical definition of this model is shown in the

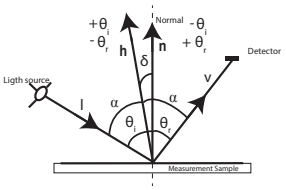

Figure 1: Angles and vectors used in Cook-Torrance BRDF model [12]

Equation (1):

$$f_r(\mathbf{l},\mathbf{v}) = k_d + k_s \frac{FDG}{\pi \cos\theta_i \cos\theta_r} \tag{1}$$

In this equation, k_d and k_s are the diffuse and specular parameters, F is the Fresnel term, D is the microfacet distribution term showing the distribution of normals w.r.t. the half vector h, G is the geometrical attenuation factor controlling shadowing and masking effect on the projected surface, and θ_i and θ_r are the angles of incidence and reflectance, respectively. For the Fresnel term, we use Schlick's approximation [13] as shown in Equation (2):

$$F = f_0 + (1-f_0)(1-\cos\theta_i)^5, \quad f_0 = \left(\frac{1-\mu}{1+\mu}\right)^2 \tag{2}$$

with μ being the material's index of refraction.

For the microfacet distribution D, we use the GGX distribution [14]. The GGX distribution represents the normal distribution probability of the microfacets, in other words, the distribution of size and direction of the microfacets. This term is shown in Equation (3):

$$D(\mathbf{h}) = \frac{{\alpha_g}^2 \chi^+(\mathbf{h}\cdot\mathbf{n})}{\pi \cos^4\theta_h \left({\alpha_g}^2 + \tan^2\theta_h\right)^2} \tag{3}$$

In this equation, θ_h is the angle between the surface normal, $\mathbf{n}$, and the half vector, $\mathbf{h}$, α_g is the width parameter of the specular lobe, and $\chi^+(x)$ equals one if x $>$ 0 and zero if x $\leq$ 0 [15]. For parameter G we use Smith's shadowing-masking function [16] and the derived equation by Walter et al. [14] which is shown in Equations (4) and (5) [15]:

$$G(\mathbf{v_i},\mathbf{v_r},\mathbf{h}) \approx G_1(\mathbf{v_i},\mathbf{h})\, G_1(\mathbf{v_r},\mathbf{h}) \tag{4}$$

$$G_1(\mathbf{v_x},\mathbf{h}) = \chi^+\left(\frac{\mathbf{v_x}\cdot\mathbf{h}}{\mathbf{v_x}\cdot\mathbf{n}}\right) \frac{2}{1+\sqrt{1+\alpha_g^2\tan^2\theta_x}} \tag{5}$$

where v_i and v_r are the unit vectors describing the incidence (i) and reflectance (r) directions, respectively. In these equations, there are parameters that we need to optimise when we are estimating the BRDF of a sample. The optimisation process can be done using different cost functions and making efforts to minimise them. Among various cost functions, three of them have been used in BRDF estimation studies, named cosine-weighted RMSE, cube root cosine-weighted RMSE [17], and the function presented by Löw et al. [18], which in this paper is called M2. These cost functions are shown in Equations (6 - 8), respectively:

$$CF1 = \sqrt{\frac{\sum\left(M(\omega_i,\omega_r)\cos\theta_i - A(\omega_i,\omega_r,p)\cos\theta_i\right)^2}{N}} \tag{6}$$

$$CF2 = \sqrt{\frac{\sum\left(\left(M(\omega_i,\omega_r)\cos\theta_i - A(\omega_i,\omega_r,p)\cos\theta_i\right)^2\right)^{1/3}}{N}} \tag{7}$$

$$M2 = \sqrt{\frac{\sum\left(\ln(1+M(\omega_\mathbf{i},\omega_\mathbf{r})\cos\theta_\mathrm{i}) - \ln(1+A(\omega_\mathbf{i},\omega_\mathbf{r},p)\cos\theta_\mathrm{i})\right)^2}{N}} \tag{8}$$

In Equations (6-8), M is the measured BRDF, and A is the estimated BRDF using the model in equation 1 with parameters p and N number of angle combinations for incident, i, and reflected, r, directions, and ω_i and ω_r are the directions of incidence and reflectance in the spherical coordinate system. The differences between the measured and estimated BRDF values are summed over all the angle combinations.

In the cosine-weighted RMSE cost function, the increase in reflectance at the grazing angles is compensated for by using the cosine weighting factor. Most of the time, RMSE functions give too much weight to the BRDF measurements at specular angles, resulting in diminishing the importance of the off-specular measurements. As an attempt to correct this issue, the cube root cosine-weighted RMSE cost function is sometimes used [17]. The logarithmic error metric, M2, gives more weight to the wide-angle scattering. Therefore, more realistic rendering can be achieved using this metric [18].

Method

This section discusses the samples and methods to measure their BRDF, the processing of the obtained data, and the BRDF optimisation approach.

Samples and Measurement

For this study, eight matt samples from various companies were chosen and are shown in Figure 2.

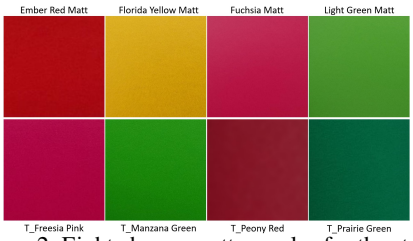

Figure 2: Eight chosen matt samples for the study

In addition to these eight samples, a Munsell white N9/ sheet was also measured as the reference white for data processing in the further steps.

The measurements were divided into two parts. In the first part, the diffuse reflections of the samples were measured using an X-Rite MA-T12 multi-angle spectrophotometer. This device enables measurements at two different viewing angles and six different illumination angles, in total, twelve measurements, each in 3 to 5 seconds. MA-T12 is equipped with a polychromatic white LED, and it measures the reflectance from 400 to 700 *nm* with 10 *nm* intervals. The measurement geometry of MA-T12 is shown in Figure 3.

In the second part, the specular measurements were performed using the Canon Surface Reflectance Analyzer RA-532H (SRA), hereby referred to as Canon SRA in the paper. With this device, it is possible to get the BRDF values at two incident angles, 20° and 60°, and viewing angles in the range of 20±2.5° and

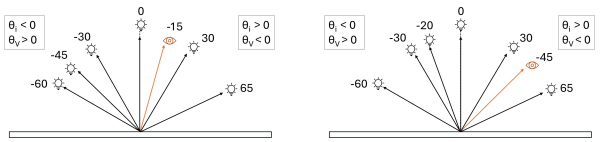

Figure 3: Measurement geometry of MA-T12: (left) Illumination angles for viewing angle at 15°, (right) Illumination angles for viewing angle at 45°

60±2.5° for each illumination angle, respectively. Among these measurements, two were chosen; one for illumination and viewing angle of 20° and the other for illumination and viewing angle of 60°. The light source is an LED light source, and the reflected light intensity is captured using an area sensor and is reported as 1D BRDF value. The duration of each measurement using this device was between 3 to 5 seconds. In total, we had fourteen different measurements, and the total duration of measurements using both devices was between 6 to 10 seconds, which compared to the traditional methods that can take up to several hours, is significantly faster [2, 5, 20].

Data Processing

The measured data obtained from the two measurement devices was normalised to compare and use it for BRDF optimisation. Measured values obtained from each device were divided by the values of the reference white sample measured using the same devices, i.e., the diffuse measurements were divided by the diffuse measurements of the reference white, and the specular measurements were divided by the specular measurements of the reference white.

Canon SRA gives the intensity of the reflected light as the 1D BRDF value; thus, there would be only one measured value for each incident and viewing angle. On the other hand, MA-T12 returns the spectral measurements of the surface reflectance. Since the goal is to fit the BRDF model on the data spectrally, it is preferred to have both the specular and diffuse measurements in the spectral domain rather than a single value. Therefore, an assumption was made based on the theory that at the specular angles, what is observed is the illumination of the source spectral power density function [19]. To process the specular part of the measurements, the intensity values obtained from Canon SRA were converted to spectral reflectance factor using Equation (9). In Equation (9), R is the spectral reflectance factor, I is the intensity, and λ is the wavelength.

$$R = \frac{I \times \pi}{\lambda_{\max} - \lambda_{\min}} \tag{9}$$

Equation (9) assumes that the reflectance factor would be constant throughout the whole spectrum, which results in a flat spectral reflectance curve but at different intensity levels for the specular measurements.

BRDF Fitting

For BRDF fitting, we used the Cook-Torrance BRDF model (CT) with the GGX distribution [14] and the measurement data. The BRDF was fitted spectrally in the range from 400 to 700 *nm* with 10 *nm* intervals.

According to the equations (1-6), for the BRDF model, 34 parameters, k_{d_λ}, k_s, α_g, and n were optimised. The aim was to

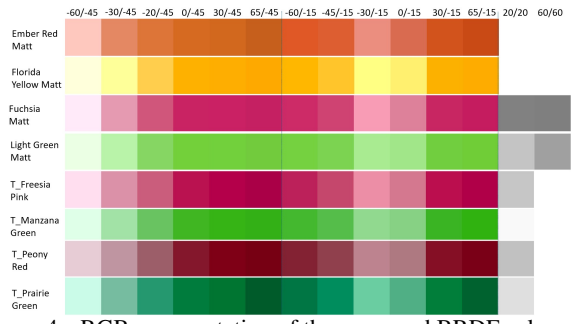

Figure 4: sRGB representation of the measured BRDF values using MA-T12 and Canon SRA for diffuse and specular measurements, respectively.

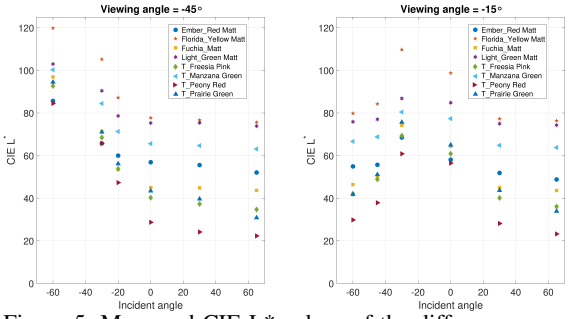

Figure 5: Measured CIE L* values of the diffuse measurements for all samples

fit a spectral BRDF, and therefore, we did use 31 parameters for the diffuse parameters, k_{d_λ} (one for each wavelength), one for the specular, k_s, one for the surface roughness which is controlled by α_g, and one for the index of refraction, n. Genetic Algorithm (GA) was used as an optimisation tool along with the measured data and three different cost functions. We expect GA to help reduce the probability of having a local minimum [20] when optimising the 34 BRDF parameters. We evaluated three different cost functions, equations (6-8), for optimising the sample BRDF parameters. The results of the optimisation and fitting process were assessed using CIEDE2000 colour difference. The CIELAB values of samples, both measured and estimated, were calculated using D65 illuminant and the 1931 standard observer.

Results and Discussion

Figure 4 shows both the diffuse and specular measurements in the sRGB colour space obtained from the two devices after the data processing steps. We can observe that the assumption of constant spectral reflectance factor throughout the spectral range for the specular measurements causes the patches to be perceived as achromatic, as only the lightness value is changed for each sample and the respective specular angle.

Figure 5 and 6 shows the CIE Lightness value (*CIE* L^*) for diffuse and specular measurements.

Estimated BRDF

The BRDF estimated at the specular angles show hue and chroma in the sRGB colour space similar to the diffuse part but with a high lightness value for all the samples, except the samples with very high lightness levels as seen in Figure 6. Figure 7 shows the sRGB representations of the measured and estimated BRDF for all the samples using three different cost functions.

Figure 6: Measured CIE L* values of the specular measurements for all samples

Figure 8 shows the measured and estimated BRDF for sample *T_Freesia pink* using three different cost functions. The flat lines are the measured reflectance at specular angles using the hypothesis mentioned earlier in the Data Processing section using Equation (9).

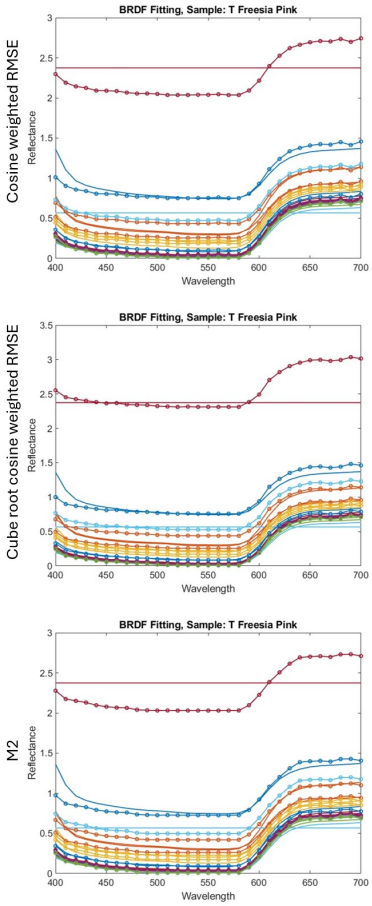

Figure 8: Measured and estimated BRDF plots for sample Freesia pink using three different cost functions. Solid lines are the measured BRDF and lines with circles are the estimated BRDF.

Figures 9 and 10 show CIE L* values of samples *T_Freesia pink* and *T_Manzana green* at two different viewing angles. These values are the measured and estimated values for the diffuse part.

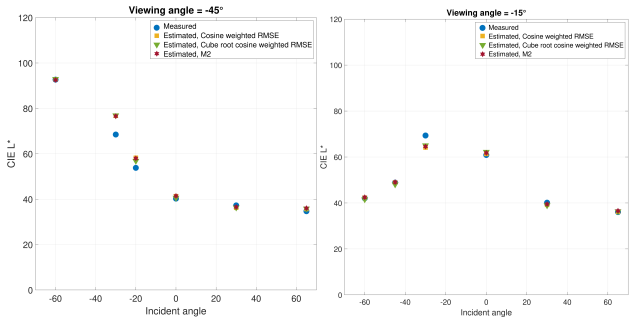

Figure 9: CIE L* values of sample T_Freesia pink at viewing angles of 45° and 15° for measured and estimated BRDF values

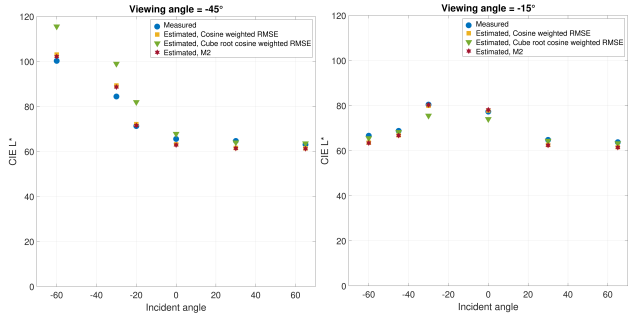

Figure 10: CIE L* values of sample T_Manzana green at viewing angles of 45° and 15° for measured and estimated BRDF values

It was observed that as the angle of incidence gets closer to the near-to-specular angles, the estimations become less accurate. This is detectable in -30°/-45° and -30°/-15° angle combinations in both plots. To have a better comprehension of the performance of the model and cost functions in estimating the BRDF measurements, the CIEDE2000 colour difference was calculated for the samples at each individual angle combination, and for all three cost functions.

The box plots of the colour differences between the measured and estimated values using each cost function are shown in Figure 11. For each sample, the colour difference was calculated for all the angle combinations, including diffuse and specular measurements, and the box plot for each sample shows both the diffuse and specular measurements. The reason behind the large observed colour differences is that we have achromatic specular measurements, but the estimated specular measurements have the same colour as the diffuse measurements for each sample due to the measurement dataset used and the GA optimisation method. This difference tends to be high; therefore, having a ground truth for the specular measurements can be helpful and can be considered for further studies. In addition, the average colour difference between the measured and estimated values across all the samples and angle combinations using various cost functions is presented in Figure 12. The boxes for each function contain colour difference information of seven samples. Sample *T_Prairie green* was excluded from this analysis because the optimisation process for this sample using the cube root cosine-weighted RMSE cost function resulted in a local minimum, despite attempts to adjust the optimisation parameters. Consequently, no estimated BRDF values were obtained for this sample using the mentioned cost function. To ensure a valid statistical comparison, *T_Prairie Green* was taken out for the other two cost functions, resulting in the same

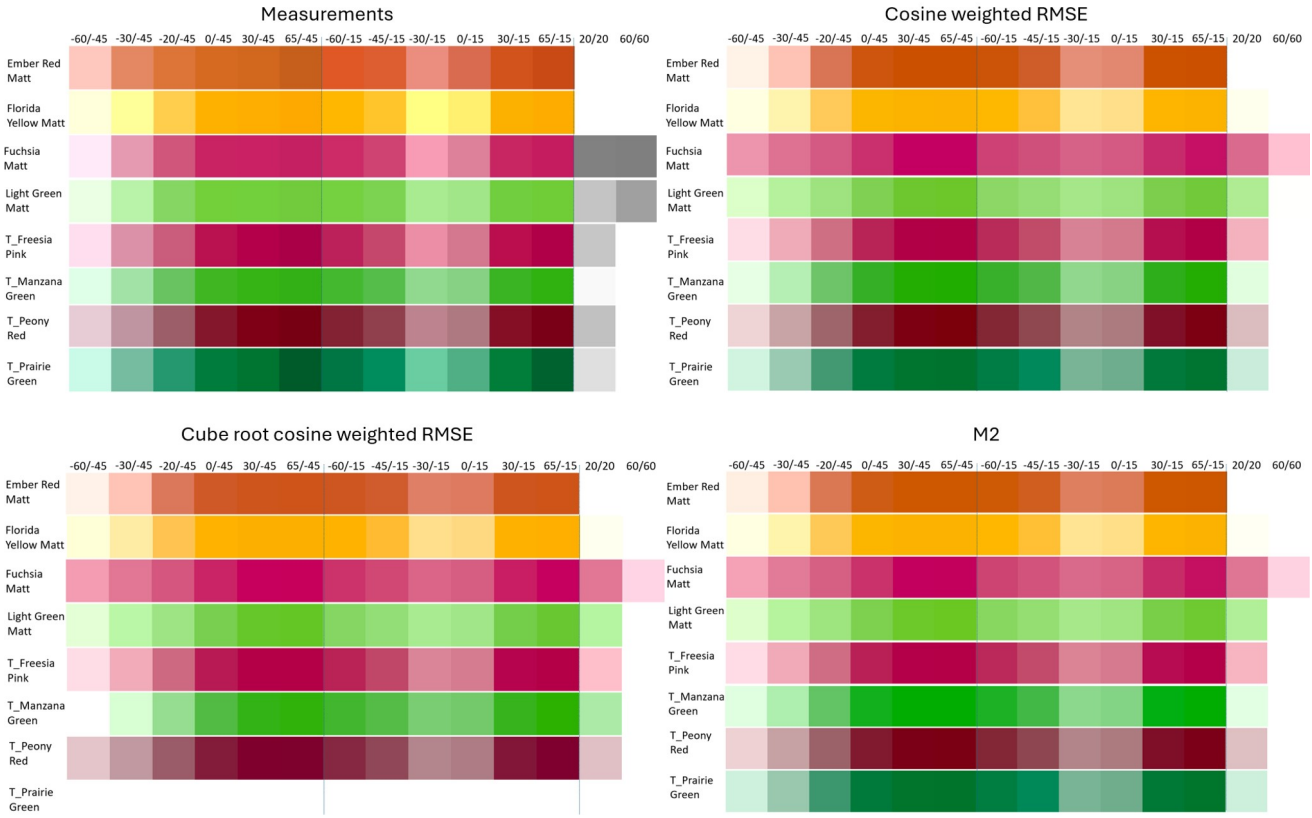

Figure 7: sRGB representations of the measured and estimated BRDF values using three different cost functions

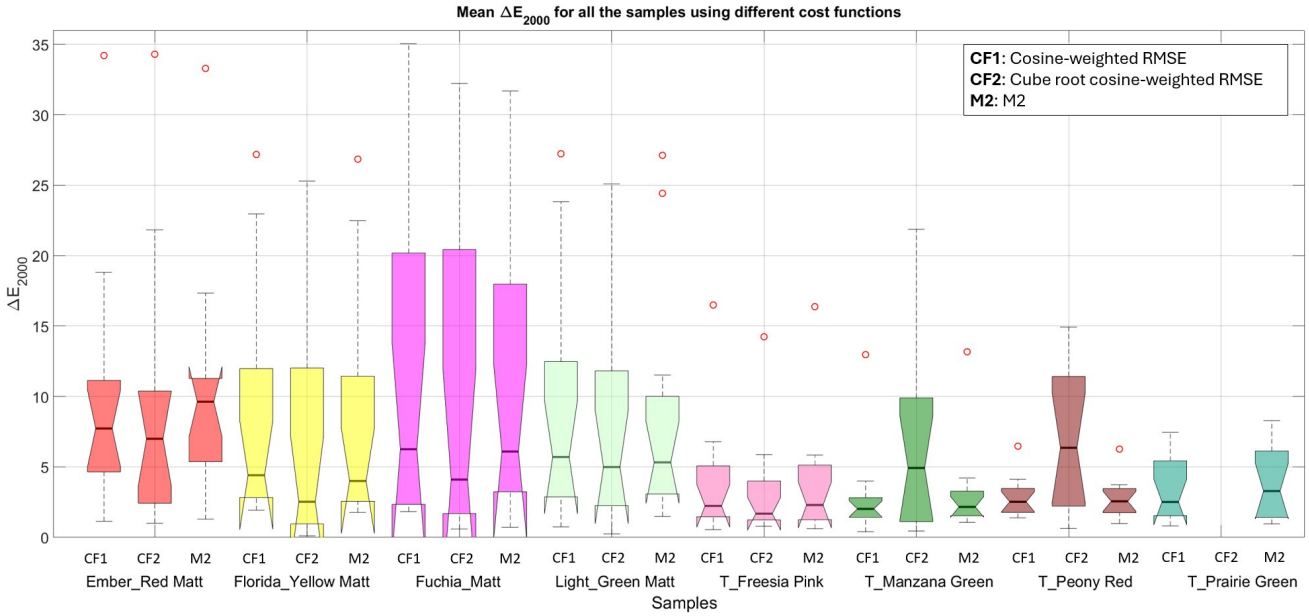

Figure 11: Box plot of colour differences between measured and estimated BRDF values using different cost functions for all the samples and all the angle combinations

number of data points for comparison.

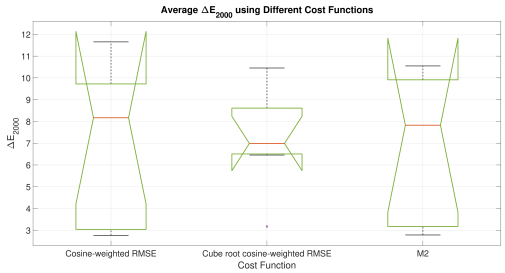

Figure 12: Average colour difference for all the samples using different cost functions

Due to the smaller confidence interval of the average colour difference for the cube root cosine-weighted RMSE (CF2), we can say that this cost function provides more consistent estimations of BRDF values. To verify the statistical significance of these results, the sign test was employed, and different cost functions were compared. The sign test is a paired, distribution-free test, which ensures the validity of the results even if our data do not follow a normal distribution [21]. The significance level, α value, was set to 0.05 during the sign test. This value indicates what the probability of rejecting the null hypothesis is when the null hypothesis is true. The p-values obtained from this test are as follows: CF1 vs. CF2: 0.189, CF1 vs. M2: 0.363, and CF2 vs. M2: 0.761. Referring to these results, with significantly large p-values, we cannot reject the null hypothesis. That is, there is no difference between the average colour differences between the measured and estimated BRDF values using three different cost functions. This can be due to the use of diffuse samples. The cost functions may show the difference in their performance when we utilise them for highly specular samples rather than diffuse ones.

Conclusion

We estimated the spectral BRDF parameters for both the diffuse and specular reflectance using the Cook-Torrance model, three different cost functions, and measurement data from two handheld devices. The results show that it is possible to use two handheld devices to perform measurements in a significantly shorter time, with lower angle combinations, and consequently, shorter processing time and lower storage usage. In addition, this method makes the optimisation and estimations possible in the spectral domain. The colour difference values between the measured and estimated values using different cost functions show that there is no significant difference between their performance since the chosen samples are all diffuse samples, and the cost functions may show varying behaviour once they are used for highly specular samples.

One of the limitations of this method is its application to highly specular samples, where the dominance of specular reflection can significantly affect the optimisation process. Therefore, developing another approach to handle specular samples could be a focus for future work. Additionally, using rendered images can be beneficial for method evaluation since they allow observation of samples under more realistic lighting conditions. Another consideration for future studies is the assumption of a flat spectral reflectance curve for specular measurements; finding methods to validate this assumption and assess its accuracy could be considered for future studies.

References

[1] F. E. Nicodemus, J. Richmond, J.J. Hsia, I.W. Ginsberg, T. Limperis, Geometrical considerations and nomenclature for reflectance, National Bureau of Standards, Washington, 160 (1977).

[2] Darya Guarnera et al., BRDF representation and acquisition, Computer Graphics Forum, 35, 2 (2016).

[3] Stephen R Marschner et al., Image-based bidirectional reflectance distribution function measurement, Applied optics, 39, 16 (2000).

[4] Wojciech Matusik, A data-driven reflectance model, PhD diss., Massachusetts Institute of Technology (2003).

[5] Addy Ngan, Durand Frédo, Matusik Wojciech, Experimental Analysis of BRDF Models, Rendering Techniques, no. 16th (2005).

[6] Radomír Vávra, Jiří Filip, Adaptive slices for acquisition of anisotropic BRDF, Computational Visual Media, 4 (2018).

[7] Dmitri Lanevski, Farshid Manoocheri, Erkki Ikonen, Gonioreflectometer for measuring 3D spectral BRDF of horizontally aligned samples with traceability to SI, Metrologia, 59, 2 (2022).

[8] Jirí Filip, Radomír Vávra, Michal Havlícek, Effective acquisition of dense anisotropic BRDF, 22nd International Conference on Pattern Recognition, IEEE (2014).

[9] Giuseppe Claudio Guarnera et al., Material capture and representation with applications in virtual reality, ACM SIGGRAPH Courses (2017).

[10] Tiancheng Sun, Henrik Wann Jensen, Ravi Ramamoorthi, Connecting measured BRDFs to analytic BRDFs by data-driven diffuse-specular separation, ACM Transactions on Graphics (TOG), 37, 6 (2018).

[11] Robert L. Cook, Kenneth E. Torrance, A reflectance model for computer graphics, ACM Transactions on Graphics (ToG), 1, 1 (1982).

[12] Aditya Sole, Image-Based Bidirectional Reflectance Measurement of Non-Diffuse and Gonio-Chromatic Materials, Doctoral thesis at Norwegian University of Science and Technology (2019).

[13] Christophe Schlick, An inexpensive BRDF model for physically-based rendering, Computer graphics forum, 13, 3 (1994).

[14] Bruce Walter, Stephen R. Marschner, Hongsong Li, Kenneth E. Torrance, Microfacet models for refraction through rough surfaces, Proc. 18th Eurographics Conference on Rendering Techniques, pg. 195. (2007).

[15] Giuseppe Claudio Guarnera, et al., BxDF material acquisition, representation, and rendering for VR and design, SIGGRAPH Asia Courses (2019).

[16] Bruce Smith, Geometrical shadowing of a random rough surface, IEEE transactions on antennas and propagation, 15, 5 (1967).

[17] Adria Fores, James Ferwerda, Jinwei Gu, Toward a perceptually based metric for BRDF modeling, Color and imaging conference, 20 (2012).

[18] Joakim Löw et al., BRDF models for accurate and efficient rendering of glossy surfaces, ACM Transactions on Graphics (TOG), 31, 1 (2012).

[19] Habib, Syeda Tanzima, Philip John Green, and Peter Nussbaum. "Estimation of BRDF measurements for printed colour samples." (2021).

[20] Aditya Sole et al., Measurement and rendering of complex non-diffuse and goniochromatic packaging materials, The Visual Computer, 37, 8 (2021).

[21] W. J Dixon, A. M. Mood, The Statistical Sign Test, Journal of the American Statistical Association, 41, 236 (1946).